Available online at www.sciencedirect.com
SCIENCE DIRECT®
Journal of Nuclear Materials 329–333 (2004) 462–466
journal of nuclear materials
www.elsevier.com/locate/jnucmat

High temperature strength of fine-grained, particle-dispersed V–(1.7–2.4)wt%Y alloys with different grain sizes and particle densities

S. Oda [a], H. Kurishita [b,*], Y. Tsuruoka [a], S. Kobayashi [c], K. Nakai [c], H. Matsui [d]

[a] Graduate Student, Ehime University, Matsuyama 790-8577, Japan
[b] International Research Center for Nuclear Materials Science, Institute for Materials Research, Tohoku University, Oarai, Ibaraki-ken 311-1313, Japan
[c] Department of Materials Science and Engineering, Ehime University, Matsuyama 790-8577, Japan
[d] Institute for Materials Research, Tohoku University, Sendai 980-8577, Japan

Abstract

In order to examine the high temperature strength of fine-grained, particle-dispersed V–Y alloys as a function of grain size and dispersed particle density, three V–(1.7–2.4)Y (in wt%) alloys were prepared by mechanical alloying and hot isostatic pressing. The alloys had grain sizes of 270–500 nm, particle size of around 15 nm and particle densities of $(1.3–7.2)\times10^{21}$ m^{-3}. The alloys, together with V–4Cr–4Ti (NIFS-Heat1), were annealed and tensile tested at room and high temperatures from 873 to 1273 K. At room temperature and up to around 1073 K, V–(1.7–2.4)Y alloys exhibited higher strengths than V–4Cr–4Ti, with strength increasing with decreasing grain size and increasing particle density. Above 1173 K, however, V–(1.7–2.4)Y alloys showed lower strengths than V–4Cr–4Ti. These results are due to a strong temperature dependence of strengths of V–(1.7–2.4)Y above 923 K compared with that of V–4Cr–4Ti. The observed mechanical behavior of V–(1.7–2.4)Y is discussed from the viewpoint of the deformation controlling mechanism.

1. Introduction

A V–4Cr–4Ti alloy with reduced contents of solute oxygen and nitrogen processed by electron-beam melting [1,2] is a primary candidate material for fusion reactor structural applications because of its inherently low-induced radioactivity, large thermal stress factor and high fracture toughness before irradiation. In order to make the alloy more attractive, it is necessary to improve both the resistance to embrittlement by irradiation and the strength at high temperatures [3–5].

The resistance to radiation embrittlement in refractory metals was shown to be improved by introducing microstructures of fine grains and finely dispersed particles [6–10]. For vanadium the authors proposed a powder-metallurgical process to reduce grain size associated with finely dispersed particles and ensure good ductility of vanadium by removing solute oxygen and nitrogen from the matrix [11]. By applying the process, they developed V–Y alloys with very fine grains and dispersed particles of Y_2O_3 and YN and demonstrated that the alloys show a good ductility and strength even in the condition of no plastic working after HIP [12] and are resistant to fast neutron irradiation at temperatures from 563 to 1073 K up to 0.25–0.7 dpa [13,14].

Since the dispersed particles of Y_2O_3 and YN were found to be thermally stable [12], they are expected to improve the high temperature strength of vanadium. In addition, fine grains can contribute to improve high temperature strength by grain boundary strengthening as far as grain boundary sliding does not occur significantly. It is thus necessary to examine how the high temperature strength of the fine-grained V–Y alloys

* Corresponding author. Tel.: +81-29 267 4157; fax: +81-29 267 4947.
E-mail address: kurishi@imr.tohoku.ac.jp (H. Kurishita).

0022-3115/$ - see front matter © 2004 Elsevier B.V. All rights reserved.
doi:10.1016/j.jnucmat.2004.04.308

dispersed with fine Y_2O_3 and YN particles depends on grain size and dispersed particle density. However, there are no reports on the high temperature strength of vanadium or its alloys with fine grains and finely dispersed particles. In this paper, fine-grained, particle-dispersed V–Y alloys are prepared with three different grain sizes and particle densities and subjected to tensile tests up to 1273 K.

2. Experimental

Powders of pure vanadium (particle size: <150 μm, oxygen: 0.08 wt%, nitrogen: 0.07 wt%), pure yttrium (<750 μm, oxygen: 1.56 wt%, nitrogen: 0.05 wt%) and Y_2O_3 (<120 μm) were used as the starting materials. They were mixed to provide the nominal compositions of V–1.7wt%Y, V–1.3wt%Y–0.8wt%Y_2O_3 and V–1.3wt%Y–1.6wt%Y_2O_3 in a glove box filled with a purified Ar gas (purity 99.9999%). Each of the mixed powders was subjected to MA in a purified Ar atmosphere: for V–1.7wt%Y a planetary ball mill with pots and balls made of WC/Co was used [12], and for V–1.3wt%Y–0.8wt%Y_2O_3 and V–1.3wt%Y–1.6wt%Y_2O_3 a three mutually perpendicular directions agitation ball mill with pots and balls made of TZM (Mo–0.5%Ti–0.1%Zr) was used [15]. HIP was conducted at 1273 K and 200 MPa for 3 h in an Ar atmosphere. From the as-HIPed compacts, specimens for microstructural observations, X-ray diffraction (XRD) analysis and tensile tests were prepared. The dimensions of the tensile specimens are 16 mm × 4 mm × 0.5 mm with the gauge section of 5 mm × 1.2 mm × 0.5 mm, where its shoulder part was designed to support the applied load [12]. All of the specimens were wrapped with Ta foil and then Zr foil and annealed at 1273 K or 1373 K for 1 h in a vacuum better than 5×10^{-5} Pa. Table 1 shows the designation and chemical compositions of the specimens subjected to annealing at 1273 K for V–2.4Y and V–1.9Y and at 1373 K for V–1.7Y. The contents of tungsten and Mo which came from the milling pots and balls due to MA are also shown.

Tensile tests were performed at room and high temperatures from 873 to 1273 K at an initial strain rate of 1×10^{-3} s^{-1} in a vacuum better than 3×10^{-4} Pa. For high temperature tensile tests, Ta and Zr foils having the dimensions identical to the tensile specimens but being cut into two parts were placed in contact with the specimens in order to suppress picking-up of gaseous interstitial impurities from the surrounding during the test. The fracture surfaces of the tensile-tested specimens were examined by scanning electron microscopy (SEM) with JSM-5400. Microstructural examinations were made by transmission electron microscopy (TEM) with JEM-2000FX operating at 200 kV. XRD analysis was made to identify the dispersed compound particles with a voltage of 30 kV and amperage of 250 mA.

3. Experimental results

3.1. Microstructure

XRD analysis showed that the clear peaks of yttrium and Y_2O_3 observed in the mixed powder completely disappeared in the MA processed powder, indicating that the yttrium and oxygen dissolved into the vanadium matrix. After HIP and anneal for each alloy clear peaks of Y_2O_3 and YN were observed as shown in the previous papers, which are due to the reaction of solute oxygen and nitrogen with yttrium during HIP [11,12].

The size distributions of grains and dispersed particles for each alloy were examined by TEM, and the average diameters of grains and dispersed particles and the number density of dispersed particles, which were determined from dark-field images, are listed in Table 2. The average grain size is decreasing and the particle density is increasing in the order of V–1.9Y, V–1.7Y and V–2.4Y, indicating that the grain size of the alloys is determined by the pinning effect of dispersed particles.

3.2. Tensile properties

Fig. 1 shows a plot of yield strength against test temperature. The ultimate tensile strength also showed

Table 2
Microstructural parameters for developed V–Y alloys

	Average grain size (nm)	Particle density ($10^{23}/m^{-3}$)	Average particle size (nm)
V–2.4Y	268	7.16	13.5
V–1.9Y	504	1.26	16.8
V–1.7Y	339	3.13	12.9

Table 1
Designation and chemical compositions of developed V–Y alloys (wt%)

Designation	Y	O	N	C	H	Mo	W
V–2.4Y	2.37	0.566	0.083	0.027	0.0001	3.35	–
V–1.9Y	1.92	0.321	0.073	0.029	0.0001	0.15	–
V–1.7Y	1.68	0.187	0.104	0.027	0.0001	–	0.272

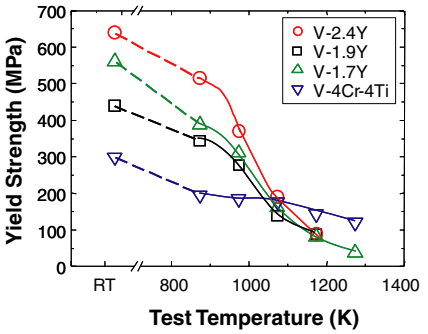

Fig. 1. Test temperature dependence of yield strength for V–(1.7–2.4)Y and V–4Cr–4Ti alloys deformed at 1×10^{-3} s^{-1}.

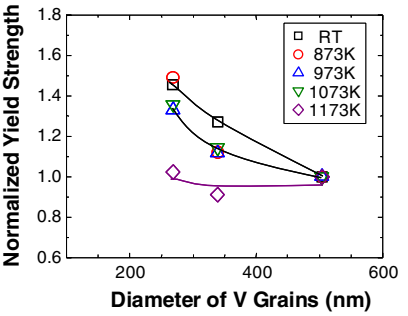

Fig. 2. Normalized yield strength as a function of grain size for V–(1.7–2.4)Y alloys deformed at various temperatures at 1×10^{-3} s^{-1}.

similar temperature dependence to the yield strength. It should be noted that up to around 1023 K the developed alloys show considerably higher strength than V–4Cr–4Ti, with strength increase in the order of V–1.9Y, V–1.7Y and V–2.4Y. In particular, the strength of V–2.4Y is approximately three times higher at 873 K and two times higher at 973 K than that of V–4Cr–4Ti. On the other hand, the yield strength of V–(1.7–2.4)Y alloys decreases significantly with increasing temperature. As a result, around 1073 K there is no significant difference in strength between V–(1.7–2.4)Y and V–4Cr–4Ti alloys, and above 1173 K V–(1.7–2.4)Y alloys exhibit lower strength than V–4Cr–4Ti.

Fig. 2 shows a plot of the yield strength against grain size for V–(1.7–2.4)Y alloys. Here, the yield strength is normalized by the yield strength at the maximum grain size, i.e., the yield strength for V–1.9Y. In the temperature range from RT to 1073 K, the normalized yield strength shows distinct and similar grain-size dependence, suggesting that the strength increases with decreasing grain size up to 1073 K, while at 1173 K the strength is almost independent of grain size.

Fig. 3 shows SEM micrographs of fracture surfaces of V–2.4Y deformed at 873 and 1173 K. The fracture surface at 873 K exhibits a dimple pattern, whereas that at 1173 K shows intergranular fracture. The fracture surface at 1073 K shows mainly a dimple pattern with partly intergranular fracture. Essentially the same results were obtained for each alloy.

Fig. 4 shows an Arrehnius plot of the yield strength for V–(1.7–2.4)Y and V–4Cr–4Ti alloys. At temperatures from around 923 to near 1173 K, the data points

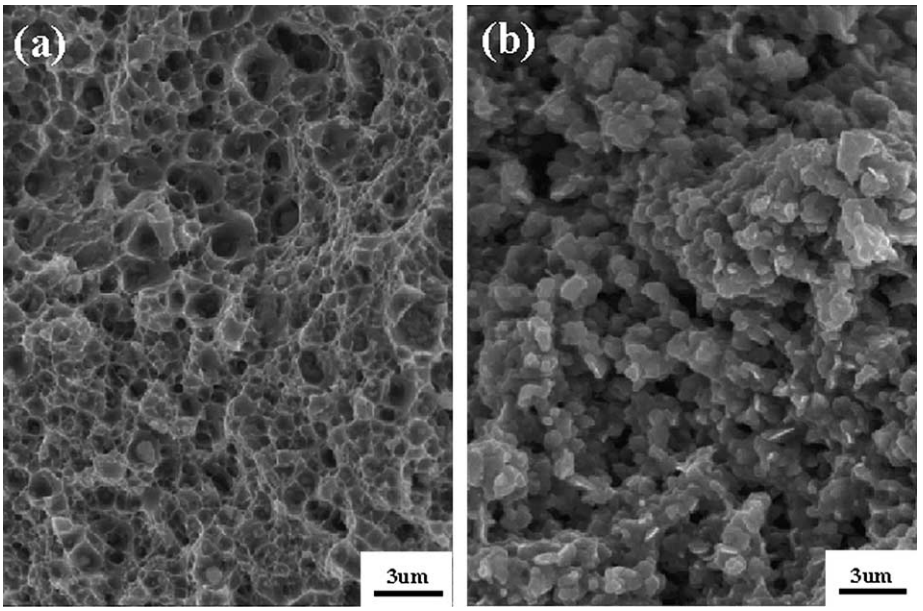

Fig. 3. SEM micrographs of fracture surfaces for V–2.4Y deformed at (a) 873 K and (b) 1173 K.

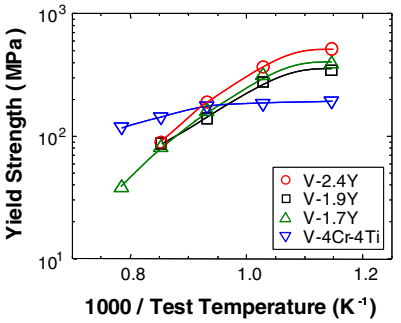

Fig. 4. Arrehnius plot of yield strength for V–(1.7–2.4)Y and V–4Cr–4Ti alloys deformed at 1×10^{-3} s^{-1}.

for V–1.7Y and V–1.9Y lie on single straight lines, whereas those for V–2.4Y provide a convex curve as a result of a significant strength decrease at 1173 K. This indicates that the deformation of V–1.7Y and V–1.9Y is controlled by a single process, while that of V–2.4Y is not controlled by a single process. In order to identify the mechanism between 923 and 1173 K for V–1.7Y and V–1.9Y, the effect of plastic strain rate on the yield strength was examined at 1073 K. It was found that the stress exponent of plastic strain rate, m, and the activation energy for deformation, Q_d, are approximately 4 and 300 kJ/mol, respectively. These values are very close to the case of high temperature deformation of bcc pure metals, where the m value is approximately 5 and the Q_d value corresponds to the activation energy for self-diffusion. In the case of pure vanadium, the activation energy for self-diffusion is reported to be 308 kJ/mol [16]. Therefore, the mechanism controlling the deformation between 923 and 1173 K for V–1.7Y and V–1.9Y is the same as that in bcc pure metals, i.e., the deformation is controlled by recovery of obstacles with a long range stress field.

4. Discussion

Considering that the highest temperature limit of V–4Cr–4Ti for the first wall structures is around 1023 K, the microstructures introduced in V–(1.7–2.4)Y alloys are very effective in improving the high temperature strength of V–4Cr–4Ti. However, above 1173 K V–(1.7–2.4)Y alloys showed lower strengths than V–4Cr–4Ti. This is due to the strong temperature dependence of the yield strength of V–(1.7–2.4)Y, compared with that of V–4Cr–4Ti. Therefore, we will discuss the cause of the strong temperature dependence of the strength in connection with the microstructures.

As shown in Figs. 1 and 4, V–(1.7–2.4)Y and V–4Cr–4Ti alloys showed similar temperature dependence of yield strength up to around 923 K, whereas above around 923 K V–(1.7–2.4)Y alloys showed larger temperature dependence of the strength than V–4Cr–4Ti, with the increasing order of V–1.9Y, V–1.7 and V–2.4Y. This corresponds to the order of decreasing grain size and increasing particle density. In general, as dispersed particle density increases, decrease in high temperature strength will be suppressed, which is opposite to the observed result. Therefore, the observed decrease in high temperature strength is attributable to the effects of grain size. The grain-size effects on strength decrease at high temperatures may be divided into two mechanisms; grain boundary sliding and recovery of long range internal stress built up inside grains. The latter increases with decreasing grain size. As was evident in Fig. 2, even at 1073 K the yield strength of V–(1.7–2.4)Y alloys showed almost the same grain-size dependence as that at 973 K, i.e., the strength increased with decreasing grain size. This indicates that even at 1073 K grain boundaries are stationary barriers against dislocation glide, i.e., grain boundary strengthening, which leads to the aspect that the deformation at 1073 K is controlled by the recovery of a long range internal field built inside fine grains. This agrees well with the deformation controlling mechanism determined from the temperature and strain rate dependence of the yield strength in the temperature range between 923 and 1173 K. On the other hand, for the deformation at 1173 K, grain boundaries had no strengthening effect, as evident in Fig. 2. This indicates that the deformation above 1173 K is due to grain boundary sliding. The occurrence of grain boundary sliding at 1173 K is also inferred by the result that the fracture surface at 1173 K was mainly intergranular. In addition, the V–2.4Y alloy which has the smallest grain size and thus is expected to possess the highest capability of grain boundary sliding exhibited a total elongation as large as 115% at 1173 K.

5. Conclusion

Three V–(1.7–2.4)Y (in wt%) alloys with fine grains and finely dispersed particles of Y_2O_3 and YN were prepared by MA-HIP processes. The microstructures of V–(1.7–2.4)Y alloys were evaluated by TEM. The alloys, together with V–4Cr–4Ti (NIFS-Heat1), were tensile tested at room and high temperatures from 873 to 1273 K at an initial strain rate of 1×10^{-3} s^{-1} and the relationship between the microstructures and high temperature strength was examined. The main results are as follows.

(1) V–(1.7–2.4)Y alloys had average grain sizes of 268–504 nm, average particle size of around 15 nm, and dispersed particle densities of $(1.3–7.2)\times10^{21}$ m^{-3}.

The grain size decreased with increasing particle density.

(2) Up to around 1023 K V–(1.7–2.4)Y alloys exhibited considerably higher strengths than V–4Cr–4Ti, indicating that the microstructures introduced in V–(1.7–2.4)Y alloys are effective in improving the high temperature strength of V–4Cr–4Ti.

(3) V–(1.7–2.4)Y alloys showed lower strengths than V–4Cr–4Ti above 1173 K, where the deformation mode has changed from a controlling process of the recovery of a long range internal stress field to the grain boundary sliding.

Acknowledgements

The authors would like to express their gratitude to Dr T. Kuwabara (presently at Sumitomo Electric Industries, Ltd.). for his contribution to a part of this study, to Dr H. Arakawa, IMR, Tohoku University, for his help with use of HIP apparatus and to Dr S. Matsuo for his reviews.

References

[1] T. Muroga, T. Nagasaka, A. Iiyoshi, A. Kawabata, S. Sakurai, M. Sakata, J. Nucl. Mater. 283–287 (2000) 711.
[2] T. Nagasaka, T. Muroga, M. Imamura, S. Tomiyama, M. Sakata, Fus. Technol. 39 (2001) 659.
[3] L.L. Snead, S.J. Zinkle, D.J. Alexander, A.F. Rowcliffe, J.P. Robertson, W.S. Eatherly, Fusion Materials Semiannual Progress Report DOE/ER-0313/23, 1997, p. 81.
[4] S.J. Zinkle, H. Matsui, D.L. Smith, A.F. Rowcliffe, E. van Osch, K. Abe, V.A. Kazakov, J. Nucl. Mater. 258–263 (1998) 205.
[5] T. Muroga, T. Nagasaka, K. Abe, V.M. Chernov, H. Matsui, D.L. Smith, Z.-Y. Xu, S.J. Zincle, J. Nucl. Mater. 307–311 (2002) 547.
[6] H. Kurishita, Y. Kitsunai, T. Shibayama, H. Kayano, Y. Hiraoka, J. Nucl. Mater. 233–237 (1996) 557.
[7] Y. Kitsunai, H. Kurishita, M. Narui, H. Kayano, Y. Hiraoka, J. Nucl. Mater. 239 (1996) 253.
[8] H. Kurishita, Y. Kitsunai, H. Kayano, Y. Hiraoka, T. Takida, T. Igarashi, in: G. Kneringer, P. Rodhammer, P. Wilhartitz (Eds.), Proceedings of the 14th International Plansee Seminar, vol. 1, 1997, p. 287.
[9] H. Kurishita, Y. Kitsunai, T. Kuwabara, M. Hasegawa, Y. Hiraoka, T. Takida, T. Igarashi, J. Plasma Fus. Res. 75 (1999) 594 (in Japanese).
[10] H. Kurishita, Basic Studies in the Field of High-Temperature Engineering, OECD, 2002, p. 103.
[11] T. Kuwabara, H. Kurishita, M. Hasegawa, J. Nucl. Mater. 283–287 (2000) 611.
[12] T. Kuwabara, H. Kurishita, M. Hasegawa, Mater. Sci. Eng., submitted for publication.
[13] S. Kobayashi, Y. Tsuruoka, K. Nakai, H. Kurishita, Mater. Trans. JIM, Mater. Trans. 45 (2004) 29.
[14] S. Kobayashi, Y. Tsuruoka, K. Nakai, H. Kurishita, these Proceedings.
[15] Y. Ishijima, H. Kurishita, K. Yubuta, H. Arakawa, M. Hasegawa, Y. Hiraoka, T. Takida, K. Takebe, these Proceedings.
[16] Metal databook, 3rd Edn., The Japan Institute of Metals, 1993, p. 24.